Article

Effect of Support on Oxidative Esterification of 2, 5-furandiformaldehyde to Dimethyl Furan-2, 5-dicarboxylate

Tingting Ge , Xiaorui Liu , Jie Tang , Chao Liu * , Jiahui Huang *

Posted Date: 13 October 2023

doi: 10.20944/preprints202310.0812.v1

Keywords: oxidative esterification; Au nanoparticles; support effects

Article

Effect of Support on Oxidative Esterification of 2, 5-Furandiformaldehyde to Dimethyl Furan-2, 5-Dicarboxylate

Tingting Ge [1,2], Xiaorui Liu [1], Jie Tang [1,2], Chao Liu [1,*] and Jiahui Huang [1,*]

[1] Dalian National Laboratory for Clean Energy, Dalian Institute of Chemical Physics, Chinese Academy of Sciences, Dalian 116023, China; getting@dicp.ac.cn (T. G.); xiaoruil@dicp.ac.cn (X. L.); jaytang@dicp.ac.cn (J. T.);

[2] University of Chinese Academy of Sciences, Beijing 100049, China;

* Correspondence: chaoliu@dicp.ac.cn (C. L.); jiahuihuang@dicp.ac.cn (J. H.);

Abstract: One-step oxidative esterification of 2, 5-furandiformaldehyde (DFF) derived from biomass to prepare Dimethyl Furan-2, 5-dicarboxylate (FDMC) not only simplifies the catalytic process and increases purity of product, but also avoids the polymerization of 5-hydroxymethylfurfural (HMF) at high temperature condition. Gold supported on a series of acidic oxide, alkaline oxide and hydrotalcite were prepared by colloidal deposition to explore the effect of support on the catalytic activities. The Au/Mg_3Al-HT catalyst exhibited the best catalytic activity in all catalysts, 97.8% selectivity of FDMC at 99.9% conversion of DFF. And this catalyst is suitable to oxidative esterification of benzaldehyde and furfural as well. X-ray diffraction (XRD), transmission electron microscopy (TEM), X-ray photoelectron spectroscopy (XPS) and CO_2 temperature programmed desorption (CO_2-TPD) were performed to characterize the catalysts. The results indicated that the medium and strong basic sites in the heterogeneous catalysts benefited for the absorption of intermediate spices, further facilitated the oxidative esterification of aldehyde groups. While, neutral or acidic support tended to aldol condensation reaction. It was worth noting that basicity on the support surface reduce electronic state of the Au nanoparticle ($Au^{\delta-}$), thus enhance the catalytic selectivity of oxidative esterification. This finding demonstrated the support plays crucial role in oxidative esterification.

Keywords: oxidative esterification; Au nanoparticles; support effects

1. Introduction

Biomass energy as the fourth largest energy after oil, coal and natural gas, is an important role in the international energy transformation. The conversion of non-edible biomass raw materials into utilizable chemicals through catalysis is one of the important ways to achieve the sustainable development of resources and friendly environment. 2, 5-furanodicarboxylic acid (FDCA) is the most promising biomass molecule to polymerization with ethylene glycol to obtain Polyethylene 2, 5-furandicarboxylate (PEF) [1], which can be used as an alternative material to polyethylene terephthalate (PET). However, due to the poor solubility of FDCA in most of industrial solvents, the conversion process of FDCA to PEF is trick [2] and it also makes the separation of FDCA to be tough via conventional purification method. Additionally, in this reaction, 5-hydroxymethyl furfural (HMF) is used as the substrate molecule, and hydroxyl group oxidation is the rate-limiting step and the process is difficult [3]. Different from FDCA, Dimethyl Furan-2, 5-dicarboxylate (FDMC) has good solubility in organic solvents. FDMC has low boiling point, which makes the FDMC easily purification by vacuum distillation as well.

There are several problems in conversion of HMF to FDMC: (1) the HMF usually contains impurities and humins, resulting in poor quality of PEF. (2) PEF showing yellow is usually caused by the decomposition of FDCA at high temperature during the polymerization of FDCA with ethylene glycol. In order to solve this problem, Jia et al. proposed to replace HMF with 2, 5-furandiformaldehyde (DFF) for oxidative esterification to prepare FDMC [3]. Compared with the

 doi:10.20944/preprints202310.0812.v1

traditional catalytic route, using DFF can not only solve the problem of low purity of product, but also avoid the oxidation of hydroxyl group to enhance catalytic activity. Therefore, the reaction process is more controllable and the cost of separation is much lower.

Au nano-catalysts have been widely used to oxidative esterification because of their unique stability [4]，especially in the HMF oxidative esterification to FDMC. In the past few decades, there have been many reports about the preparation of FDMC on Au nanoparticles. Supported gold catalysts have high activity to the oxidation of aldehyde group [5], the HMF turnover frequency on Au ranged from 2 to 5 s^{-1}. Huo et al. constructed the Au-ZrO_x interface and obtained 99.4% yield of FDCA by modulating the crystalline phase structure of ZrO_2, proving that the electron transfer between Au and ZrO_2 is conducive to promoting the adsorption of O_2 [6]. Transition metal oxide modified Au/TiO_2 catalyzed the oxidative esterification of HMF, 100% HMF conversion and more than 90% FDCA yield could be obtained, showing that the electron-rich $Au^{\delta-}$ on the catalyst surface enhanced the interaction between reactants and catalysts [7].

The synthesis of FDMC usually required an alkaline environment. Under alkaline conditions, Au/TiO_2 [8] and Au nanoparticles-sPSB [9] could convert HMF to FDMC with 98% yield. However, in the absence of alkaline additive, Au is easily deactivated due to the effect of carboxylic acid intermediates [10]. At the same time, another problem that needs to be concerned about is the presence of excessive alkaline additives (such as NaOH) not only lead to the increase of salt by-products and the rise of separation costs, but also destroy the active site on the catalyst surface. Therefore, alkaline supports are often used as a potential alternative to alkaline additives. Song et al. used organic base group-grafted silica aerogel supported Au to catalyze oxidative esterification of furfural, and the yield of methyl furoate could be above 98% [11]. Ferraz used Au/MgO catalyst in oxidative esterification of furfural, achieving a methyl furoate yield of 95% [12]. In the process of alcohol oxidation catalyzed by heterogeneous catalysts, the adsorption of substrates on the active site usually determines the reaction mechanism and product selectivity [7].

Although there have been a lot of progress on the preparation of FDMC via oxidative esterification of HMF, there is still a little work on the preparation of FDMC through oxidative esterification of DFF. In this paper, we used DFF as raw material and Mg-Al hydrotalcite supported gold as catalysts to obtain FDMC via a one-step oxidative esterification process. We investigated the effects of support acid-base property and the electron state of Au on catalytic activity.

2. Results and Discussion

2.1. Catalysts characterization

XRD pattern of several basic oxides and hydrotalcite supported Au catalysts were characterized in Figure 1. The diffraction peaks in all the samples were able to agree well with the PDF cards of the supports. Of note, the XRD diffraction angle of Mg_2Al-HT shifted to a smaller angle after the Mg-Al molar ratio was reduced to 2:1, indicating that the layer spacing of the hydrotalcite structure became larger and the increase of aluminum content. No diffraction peaks appeared for gold, showing the size of Au nanoparticles is small. TEM images displayed the mean size distribution of gold nanoparticles on the surface of different catalysts in Figure 2. The mean size of gold nanoparticles was uniformly distributed about 5-6 nm, which confirmed the four types supports hardly affect the size of Au nanoparticles. ICP-OES tested the Au content in supported catalyst, and the content of Au was 0.39 wt%.

Preprints (www.preprints.org) | NOT PEER-REVIEWED | Posted: 13 October 2023 doi:10.20944/preprints202310.0812.v1

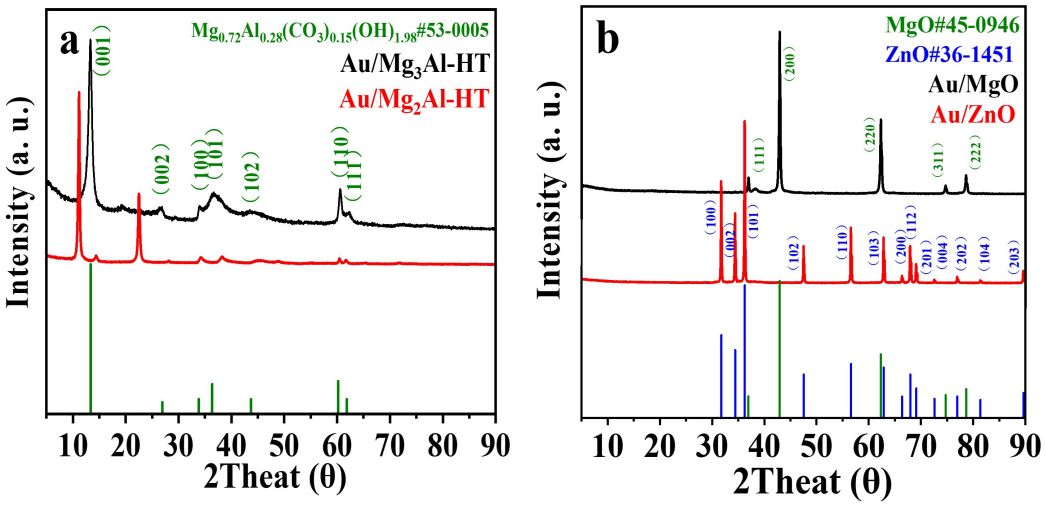

Figure 1. (**a**) XRD pattern of Au/Mg_3Al-HT and Au/Mg_2Al-HT, (**b**) Au/MgO and Au/ZnO.

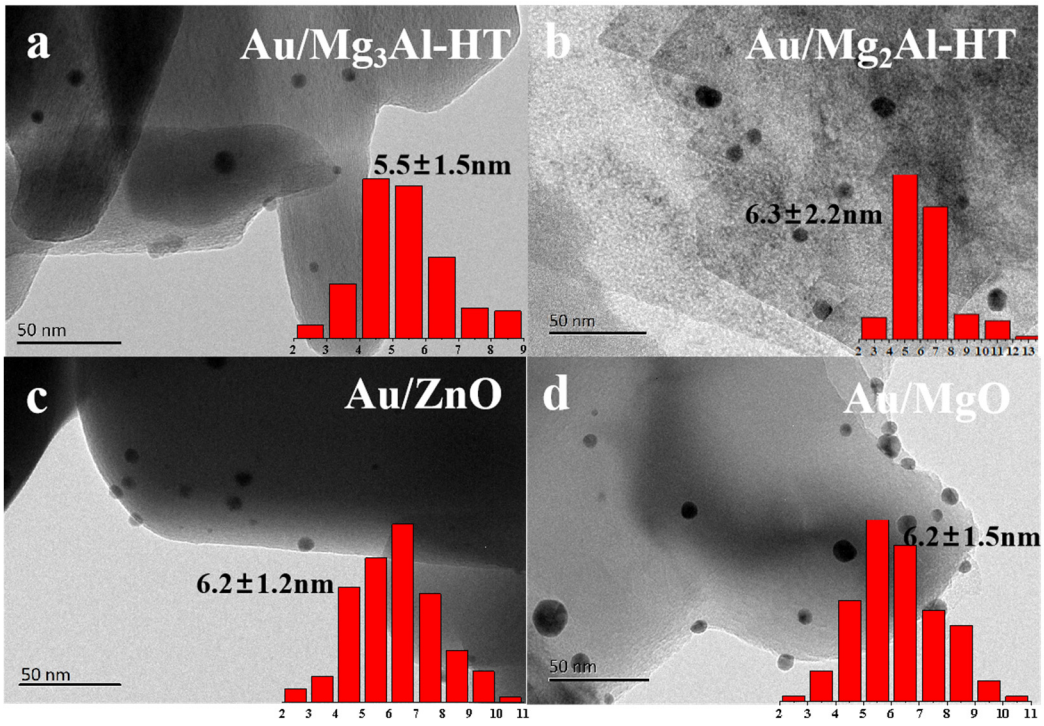

Figure 2. TEM image of (**a**) Au/Mg_3Al-HT, (**b**) Au/Mg_2Al-HT, (**c**) Au/ZnO, (**d**) Au/MgO. Inset shows the particle size distribution of Au nanoparticles.

Catalytic performance of a series of oxide and hydrotalcite supported Au catalysts were tested in oxidative esterification of DFF. The reaction was conducted at 140 °C and 2 MPa air for 8 h. The possible conversion paths for oxidative esterification of DFF in methanol are listed in Scheme 1. According to the catalytic performance, these catalysts, that was, Au/SiO_2, Au/TiO_2, Au/CeO_2, Au/ZrO_2 and Au/Al_2O_3, showed 80% selectivity of bis(dimethoxymethyl)furan (BDM) and 20% selectivity of 5-(dimethoxymethyl) furan-2-carbaldehyde (FFDM) at complete conversion of DFF (Figure 3). La_2O_3 and ZnO supported Au catalysts had high yield of FDMC (74.6% for Au/La_2O_3, 83.8% for Au/ZnO) under 99% conversion of DFF, and the by-product was methyl 5-(dimethoxymethyl) furan-2-carboxylate (DMME). Au/Mg_3Al exhibited the best catalytic activity with 97.8% selectivity of FDMC at 99% conversion. It was worth noting that when the Mg-Al ratio was 2:1, the selectivity of FDMC and carbon balance of the reaction would decrease significantly. The amount of reactants lost was 49.5%, and only 42.4% of 5-(methoxycarbonyl) furan-2-carboxylic acid (MECA)

Preprints (www.preprints.org) | NOT PEER-REVIEWED | Posted: 13 October 2023 doi:10.20944/preprints202310.0812.v1

was collected. Similar to Au/Mg_2Al-HT, significant carbon loss (34.3%) was also found on the Au/MgO catalyst. Due to the high carbon loss, Au/MgO had a 99% selectivity for FDMC, but the yield of the target product was only 65.7%. Therefore, these activity experiment directly reflected the influence of supports on product selectivity. In general, those catalysts with base sites (Au/Mg_3Al-HT, Au/Mg_2Al-HT, Au/ZnO, Au/MgO and Au/La_2O_3) allowed to obtain oxidative esterification products, while catalysts with acid sites could only obtain aldol condensation products after the reaction [13]. According to literature [2], basic supports could encourage the hemiacetal converted to ester, but acidic supports prefer to convert hemiacetals to acetals, which is a reversible process. In oxidative esterification of DFF, the presence of base sites is crucial for promote DFF oxidative esterification. Additionally, different basicity of the supports would affect the carbon balance of the reaction and the reaction intermediates of esterification. We detected the presence of magnesium salts in the solution after reaction, indicating the loss of magnesium of the supports could hinder the further esterification of the intermediate products (carboxylic acids). The reaction intermediates reacted with magnesium ions to form salt, further led to the carbon loss.

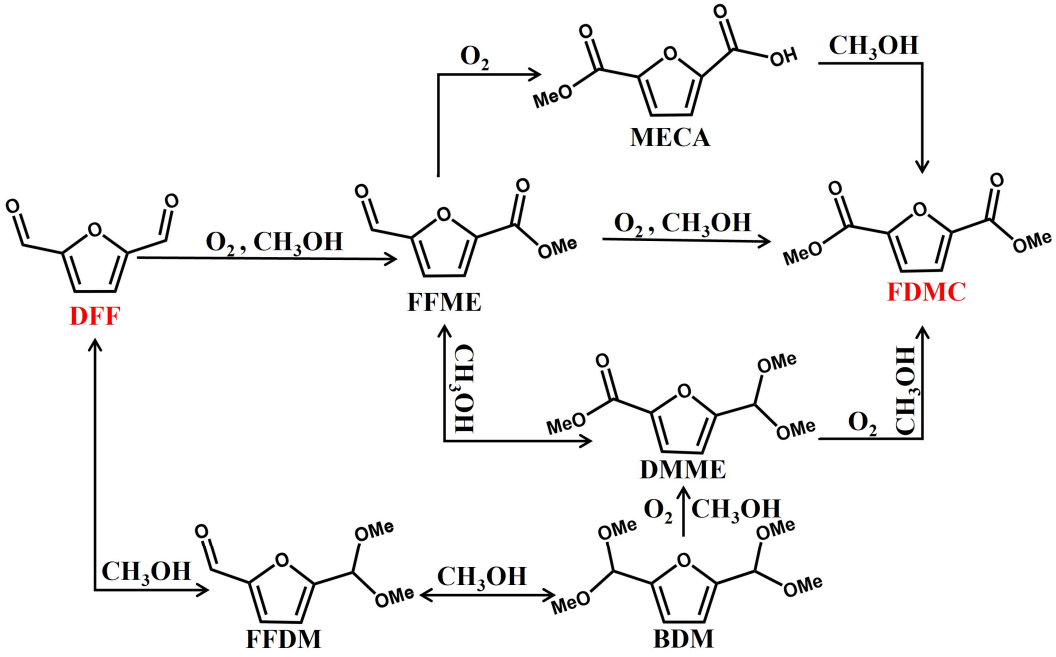

Scheme 1. Possible reaction paths of oxidative esterification of DFF in methanol.

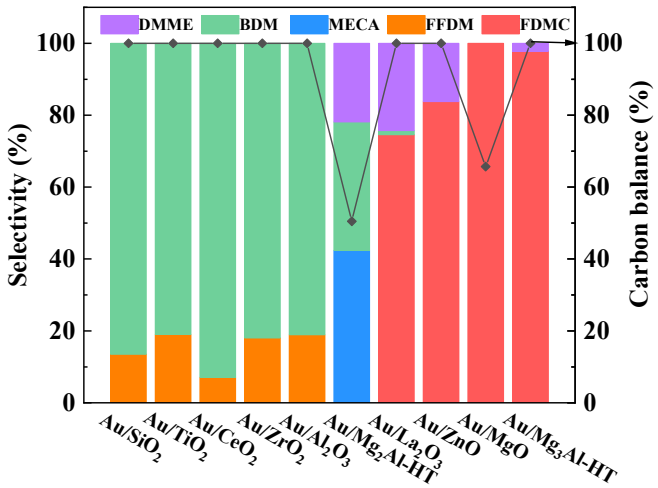

Figure 3. Oxidative esterification of DFF over Au catalysts with different supports.

Preprints (www.preprints.org) | NOT PEER-REVIEWED | Posted: 13 October 2023 doi:10.20944/preprints202310.0812.v1

In order to characterize the strength of alkalinity on different supports. CO_2-TPD analysis was carried out on the basic supported Au catalysts. In Figure 4a, Au/Mg_3Al-HT showed the maximum desorption quantity of CO_2 between 350-600 °C, and Au/La_2O_3 showed obvious CO_2 desorption signal between 600-800 °C. For Au/Mg_2Al-HT, Au/MgO and Au/ZnO, the temperature between 250-600 °C showed very weak signals. Corresponding to the different CO_2 desorption temperature, the basic sites on the catalyst surface can be divided into weak basic sites (<250 °C), medium basic sites (250-400 °C), strong basic sites (400-600 °C) and super basic sites (>600 °C) [13]. It is commonly acknowledged that the weakly basic site was provided by the -OH group on the surface of catalysts for the formation of hydrogen bonds, the medium basic site was provided by M-O pairs, and the strong basic site was from lattice oxygen [14]. Furthermore, considering the possible presence of acidic sites on the catalysts surface, we performed NH_3-TPD to test on these five catalysts. In Figure 4b, Au/Mg_3Al-HT also showed the strongest NH_3 desorption signal between 400-600 °C. For Au/Mg_2Al-HT, Au/MgO, Au/ZnO and Au/La_2O_3, they all showed similar weak NH_3 signal.

According to the catalytic results, Mg_3-Al_1 hydrotalcite catalyst exhibits significantly higher CO_2 and NH_3 adsorption capacity. It is generally believed that the acidic site on the catalyst surface is conducive to the adsorption and polarization of aldehyde groups of DFF [15], further promotes the nucleophilic attack of methanol to form hemiacetal intermediates. In present of alkaline sites, hemiacetal intermediates are more inclined to bind with Au on the catalyst surface to promote the formation of esters [12]. Au/La_2O_3 showed a strong CO_2 desorption signal above 600 °C, but with a very weak NH_3 adsorption capacity, the yield of FDMC is only 74.6%. Au/Mg_2Al-HT, Au/MgO and Au/ZnO had similar CO_2 and NH_3 desorption patterns, but these catalysts exhibited different catalytic activities. Au/Mg_2Al-HT produced a large amount of acetal products (57.6%). Au/MgO led to a significant amount of carbon loss (34.3%). In contrast, Au/ZnO could obtain a FDMC yield of more than 80% (Figure 3). Based on these results, the number of medium & strong alkaline sites and appropriate acidic sites had an effect on catalyst activity in oxidative esterification.

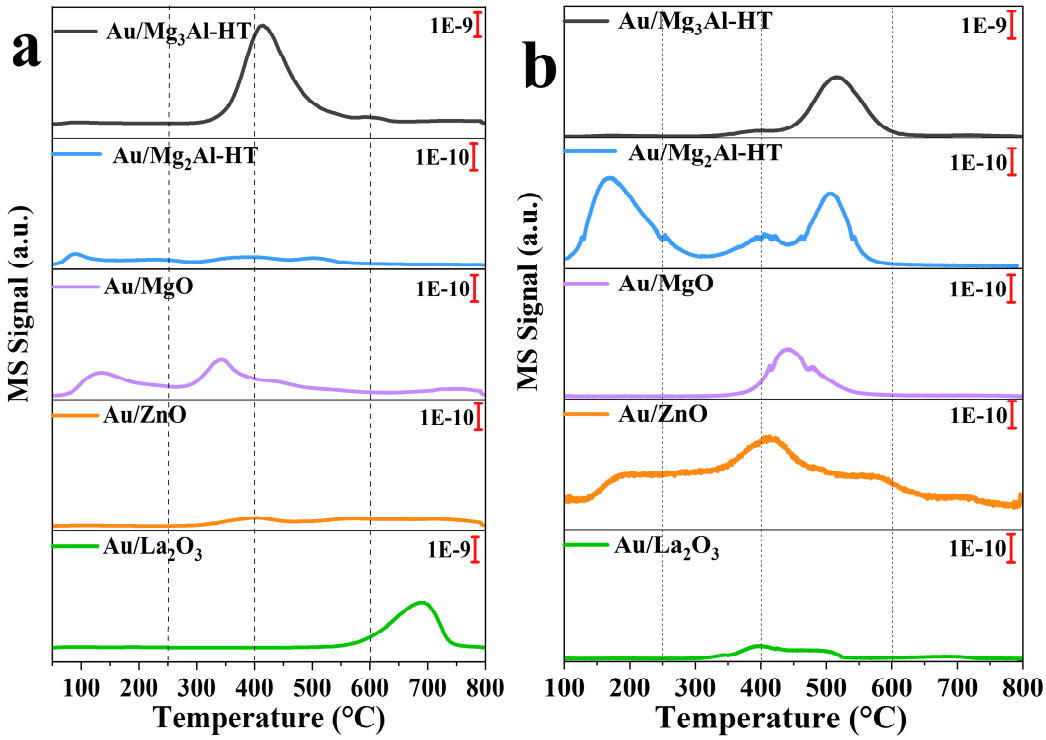

Figure 4. (**a**) CO_2-TPD; (**b**) NH_3-TPD desorption profile obtained for Au/Mg_3Al-HT, Au/Mg_2Al-HT, Au/ZnO, Au/MgO and Au/La_2O_3.

In order to further determine the correlation between the electron states of Au on the catalyst surface and the catalytic activity of the catalyst, XPS characterization were carried out on gold

Preprints (www.preprints.org) | NOT PEER-REVIEWED | Posted: 13 October 2023 doi:10.20944/preprints202310.0812.v1

catalysts with those five alkaline supports, and the results were shown in Figure 5. It was noteworthy that on the surface of several alkaline supports, the electron binding energy of the Au $4f_{7/2}$ shifted to a lower binding energy than that of the metallic Au (84.0 eV). Au on Au/Mg_3Al-HT had the lowest Au $4f_{7/2}$ electron binding energy (83.32 eV), followed by 83.42 eV for Au/ZnO, 83.63 eV for Au/La_2O_3, 83.78 eV for Au/MgO, and 84.05 eV for Au/Mg_2Al-HT, which was consistent with the catalytic activity of the catalyst, indicating that higher electron density is favorable for DFF oxidative esterification The stronger electron transfer between Au and the carrier makes $Au^{\delta-}$ more active for the activation of C-H bonds in DFF [16], benefiting to the formation of ester.

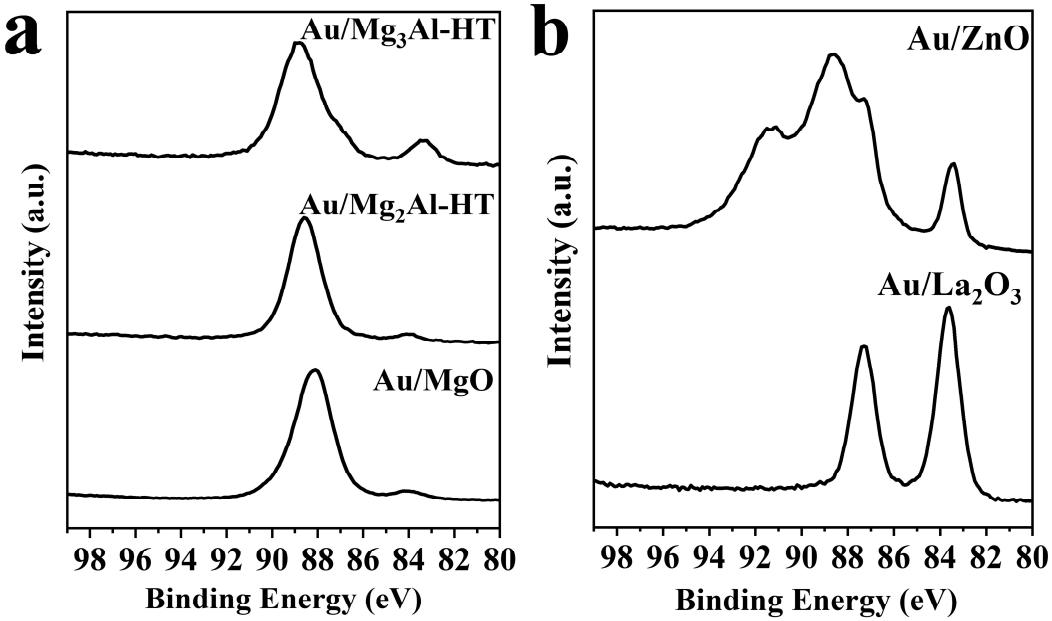

Figure 5. XPS spectra of (**a**) Au/Mg_3Al-HT, Au/Mg_2Al-HT and Au/MgO; (**b**) Au/ZnO and Au/La_2O_3.

2.2. Effect of calcination temperature of catalyst

The effect of calcination temperature on the yield of FDMC was discussed. Different calcination temperatures usually affect the exposure of active sites on the surface of catalysts and the dispersion of active metal components [17]. Au/Mg_3Al-HT catalysts were treated for 2 h at 200 °C, 300 °C and 500 °C respectively. As shown in Figure 6a, the relationship between the yield of FDMC and the calcination temperature of catalyst presented a volcanic curve. The catalyst without heat treatment had low activity (92.9% of DFF conversion, 27.8% selectivity for FDMC and 65.1% for methyl 5-formylfuran-2-carboxylate (FFME)). After calcinating at 200 °C, 69.7% FDMC could be obtained with 20.4% DMME. When the calcination temperature was 500 °C, the reaction results (83.4% of the conversion, 25.8% selectivity for FDMC and 35.4% for FFME) was close to the results of Au/Mg_3Al-HT without heat treatment. After calcining at 300 °C, the catalyst could achieve more than 99.9% conversion and 97.8% yield of FDMC. These results demonstrated that proper calcination temperature can expose active sites of Au nanoparticles and inhibit the aldol condensation reaction.

2.3. Effect of reaction temperature

The confirmation of the catalyst with the best catalytic activity prompted us to screen for the best reaction conditions. In the oxidative reaction, the reaction temperature usually has a significant impact on the conversion rate of the substrate. Au/Mg_3Al-HT catalyst was used to catalyze the oxidative esterification of DFF with methanol at 120 °C, 140 °C and 160 °C respectively. In Figure 6b, under 160 °C, the high reaction temperature led to the increase of aldol condensation products (88.4% for FDMC, 10.3% for DMME with trace MECA and BDM). When the reaction temperature decreased to 120 °C, the FDMC yield was 84.7%, with 8.3% FFME and 7.0% DMME. At 140 °C, the highest FDMC

Preprints (www.preprints.org) | NOT PEER-REVIEWED | Posted: 13 October 2023 doi:10.20944/preprints202310.0812.v1

yield is 97.8% and only 2.2% DMME was obtained. These results indicated that overhigh reaction temperature is conducive to the improvement of the activity of acidic sites, leading to the increase of aldol condensation. The other hand, due to the limitation of reaction energy barrier, decreasing reaction temperature would lead to the increase of monoester products [18].

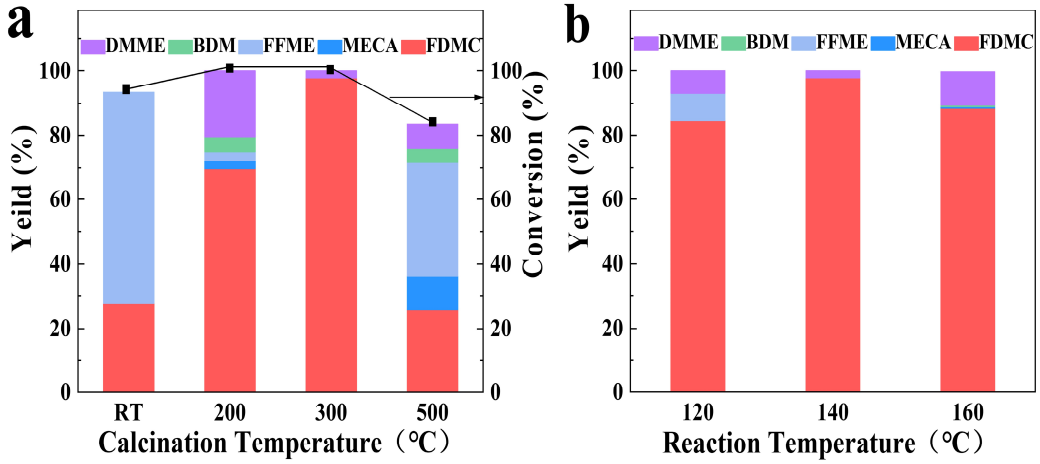

Figure 6. (**a**) Oxidative esterification of DFF on Au/Mg$_3$Al-HT catalyst with different calcination temperature, (**b**) Oxidative esterification of DFF at different reaction temperature using Au/Mg$_3$Al-HT catalyst.

We plotted the reaction time curve of DFF oxidative esterification on Au/Mg$_3$Al-HT catalysts, by collecting the reaction products at different reaction stages (Figure 7). After 1 hour of reaction, the yield of FDMC is 31.1%, with 95.7% conversion of DFF. The yield of FDMC showed a slightly decrease after 3 hours. And then FDMC gradually increased with the extension of time. During the reaction, the yield of detectable by-products always maintained below 20%. After 8 hours of reaction, DMME was the only by-product, with a yield of 2.22%.

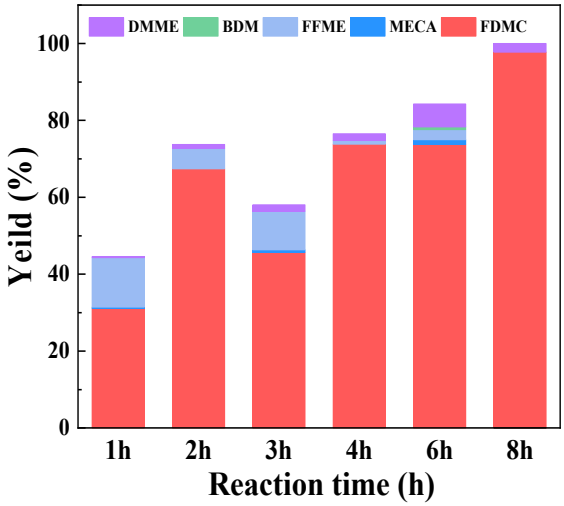

Figure 7. Oxidative esterification of DFF using Au/Mg$_3$Al-HT catalyst with different time.

2.4. Catalytic performance of Au/Mg$_3$Al-HT on different substrates

We investigated the catalytic ability of Au/Mg$_3$Al-HT catalyst to oxidative esterification of different aldehyde substrates, including benzaldehyde and furfural. As shown in Table 1 (entry 1, 2), the catalyst showed high activity for the reactants with single aldehyde groups as well. The yield of corresponding esters could achieve more than 97%. When different kinds of fatty alcohols were used as solvents for oxidative esterification of DFF (Table 1, entry 3-6), it was evident that the conversion

Preprints (www.preprints.org) | NOT PEER-REVIEWED | Posted: 13 October 2023 doi:10.20944/preprints202310.0812.v1

of DFF and the yield of esterification products steadily decline as the carbon atom of the solvent increasing. The larger steric hindrance of alcohols impeded the esterification process. At the same time, the products of solvents self-oxidative polymerization gradually increased. Higher activity of hydrogen atoms in hydroxyl and smaller steric hindrance makes methanol easier to esterification.

Table 1. Oxidative esterification of different substrates using Au/Mg_3Al-HT catalyst.

Entry	Substrate	Solvent	Conv.	(di)ester	monoester	monoacetal	monoester monoaceta	(di)acetal
entry 1	FF [1]	methanol	100.00	97.23	/	/	/	2.77
entry 2	BzH [2]	methanol	100.00	99.01	/	/	/	0.99
entry 3	DFF	methanol	100.00	97.78	/	/	/	2.22
entry 4	DFF	ethanol	100.00	54.61	12.89	6.47	24.45	1.57
entry 5	DFF	n-butanol	94.02	6.65	3.76	82.59	6.99	/
entry 6	DFF	1-pentanol	59.24	/	2.60	34.56	62.84	/

[1] Furfural. [2] Benzyl alcohol. Reaction condition: Substrate: Au= 200: 1; Solvent: 15 ml; Atmosphere: air, 2 MPa; Reaction time: 8 h; Reaction temperature: 140 °C.

2.5. Stability of Au/Mg_3Al-HT catalyst

To evaluate the catalyst stability, the catalytic activity of Au/Mg_3Al-HT-Used was tested under the same reaction conditions. The results showed that the activity of Au/Mg_3Al-HT catalyst decreased significantly, with 99.9% conversion and 73.7% selectivity. To explore the reasons of catalyst deactivation, the Au loading of the catalyst after reaction was tested by ICP-OES, the metal load remained essentially constant at 0.3786 wt%, indicating that there was no significant loss of the Au active component. XRD pattern showed the structure of the catalyst did not significantly change for used catalyst. But the diffraction peak intensity of the hydrotalcite (001) surface decreased, illustrating that the loss of magnesium during the reaction, leading to the deformation of the surface structure of the support. At the same time, the peak intensity of the (111) and (311) planes of Au increased after the reaction, proving that the size of Au nanoparticles slightly increased [19] (Figure 8a). The TEM image also confirmed that Au nanoparticles on the catalyst surface increased from 5.5 nm to 6.8 nm after first cycle (Figure 8b). XPS characterization showed the binding energy of $Au4f_{7/2}$ of used catalyst was still at 83.31 eV (Figure 8d). These characterization results showed that the loss of the support basic site might be the primary factor to deactivation of catalysts.

Preprints (www.preprints.org) | NOT PEER-REVIEWED | Posted: 13 October 2023 doi:10.20944/preprints202310.0812.v1

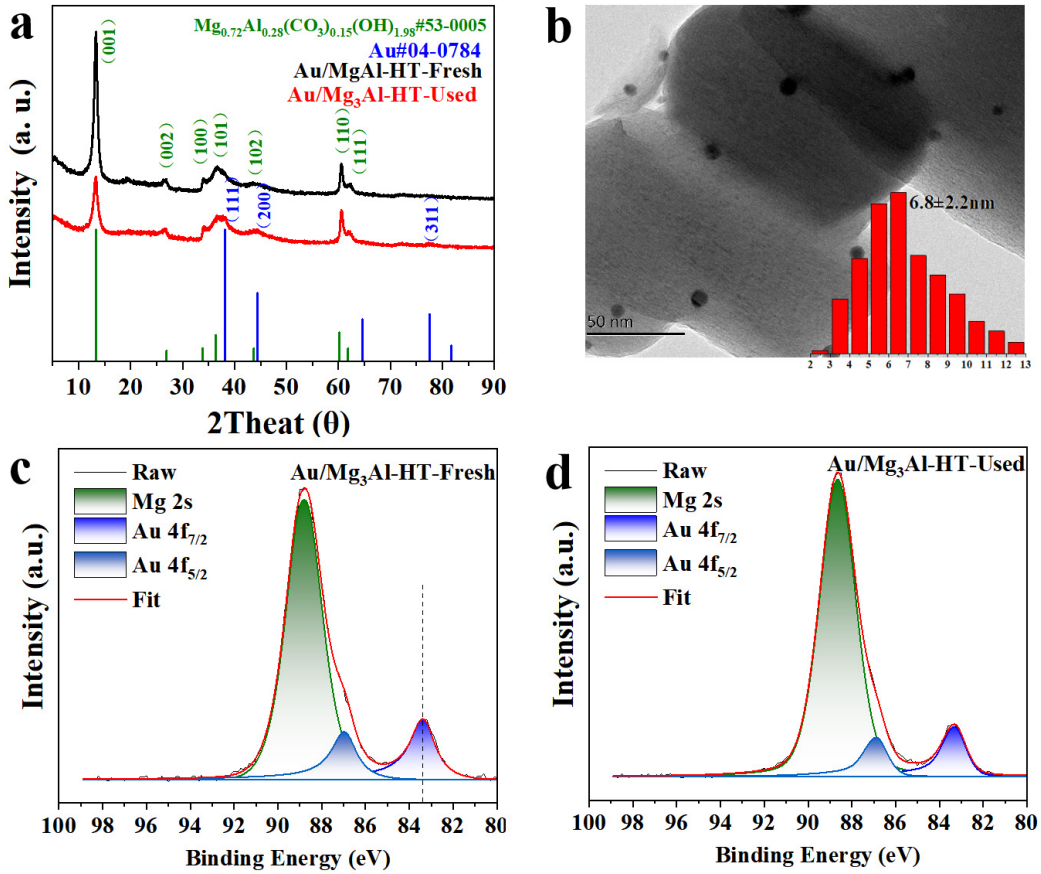

Figure 8. (**a**) XRD pattern of Au/Mg_3Al-HT-Fresh and Au/Mg_3Al-HT-Used, (**b**) TEM image of Au/Mg_3Al-HT-Used; (**c**) XPS Spectra of Au/Mg_3Al-HT-Fresh and (**d**) Au/Mg_3Al-HT-Used.

3. Materials and Methods

3.1. Materials

Tetrachloroauric(III) acid ($HAuCl_4{\cdot}4H_2O$, >99.99% metals basis, Sinopharm Chemical Reagent Co., Ltd.), Polyvinylpyrrolidone (average M.W. 8000, K16-18), Sodium borohydride ($NaBH_4$, >98%, Sinopharm Chemical Reagent Co., Ltd.), Aluminium oxide (Al_2O_3, >99.99% metals basis, 40 nm, MACKLIN), Hydrotalcite ($Al_2Mg_6{\cdot}CO_3{\cdot}16(OH){\cdot}4(H_2O)$, >98%, HEOWNS), Magnesium oxide (MgO, AR, Kermel), Zinc oxide (ZnO, AR, Kermel), Lanthanum oxide (La_2O_3, AR, Kermel), Zirconium dioxide (ZrO_2, >99.0%, Sinopharm Chemical Reagent Co., Ltd.), Cerium oxide (CeO_2, AR, Kermel), Titanium(IV) oxide (Aeroxide P25, ACROS ORCANICS) Magnesium nitrate hexahydrate ($Mg(NO_3)_2{\cdot}6H_2O$, AR, Kermel), Aluminum nitrate nonahydrate ($Al(NO_3)_3{\cdot}9H_2O$, AR, Sinopharm Chemical Reagent Co., Ltd.), Urea (CH_4N_2O, AR, Sinopharm Chemical Reagent Co., Ltd.), Methyl alcohol (CH_3OH, AR, Sinopharm Chemical Reagent Co., Ltd.), Ethanol (CH_3CH_2OH, AR, Sinopharm Chemical Reagent Co., Ltd.),

3.2. Preparation of the catalyst

Preparation of Mg_2Al-HT support: Magnesium aluminum hydrotalcite (Mg_2Al-HT) was prepared by precipitation deposition method, referring to the literature [20]. Magnesium nitrate hexahydrate (20 mmol) and aluminum nitrate hexahydrate (10 mmol) were dissolved in 200 ml deionized water. Then the pH of the solution was adjusted to 12 by dropwise adding ammonium hydroxide, stirring at room temperature for 20 min. The reaction stands at room temperature for 1 h, and then the precipitation was centrifuged and washed with water three times. The precipitation was dispersed in 70 ml deionized water and transferred to a polytetrafluoroethylene reactor at 140 °C for

 doi:10.20944/preprints202310.0812.v1

72 h. After the reaction, the product was centrifuged and dried. The product was calcined at 200 °C for 2 hours to remove the water molecules of the hydrotalcite.

Preparation of Au/Mg_3Al-HT catalyst: Supported gold catalysts were prepared by colloidal deposition method. 11 mg chlorauric acid tetrahydrate was dissolved in 45 ml anhydrous ethanol, 70 mg polyvinylpyrrolidone (Mw = 8000) was added into above solution. After 30 min, alcohol solution of sodium borohydride (2.1 mg sodium borohydride dissolving in 2.5 ml ethanol) was quickly introduced into the reaction solution. The solution color fleetly changed from light yellow to wine red, and the reaction continued for 1 h at room temperature. Au nanoparticles were diluted by addition of twice volume ethanol. Following, 529 mg of Mg_3Al-HT was added into Au solution. The precipitation was centrifugated and dried in vacuum for 12 h. After calcination at 300 °C for 2 h, Au/Mg_3Al-HT catalyst was obtained. Other supported Au catalysts with different oxides were prepared following the same method. The theoretical loading of the metal for all catalysts was 1 wt% (the actual metal load was 0.394 wt% according to ICP-OES).

3.3. Catalytic evaluation

One-step oxidative esterification of DFF to FDMC was carried out in a stainless-steel high-pressure reactor. 33.2 mg DFF, 15 ml methanol, 26.2 mg cat., 100 μL dodecane (internal standard substance) were put into the reactor, and 2 MPa air was filled after sealing the reactor. In 30 minutes, the reactor temperature rose to 140 °C, the magnetic stirring speed was set at 1000 rmp, and the reaction time was 8 h. After the reaction, the reactor was quickly transferred to cold water to cool down. The reaction products were analyzed by GC-MS (GC, Agilent 7890 A), equipped with HP-5 (30 m, 0.32 mm).

4. Conclusion

A series of oxide and hydrotalcite supported gold catalysts were prepared for catalyzing DFF oxidative esterification to FDMC. The catalytic performance demonstrated that basic supports made the catalysts more active for oxidative esterification. When using Mg_3Al-HT as the catalyst support, FDMC yield achieved to 97.8%. The Au/Mg_3Al-HT also exhibited outstanding catalytic performance to oxidative esterification of others aldehyde substrates. According to CO_2-TPD and XPS characterization, the concentration of alkaline sites on the catalyst surface and the electronic structure of Au both had an important impact on the catalytic activity. It was found that the loss of alkaline sites caused by the fall off of magnesium from the support during the reaction is a major factor of catalyst deactivation. Therefore, there are still problems of the stability of the support to be solved.

Author Contributions: Conceptualization, T.G.; methodology, T.G. and X.L.; software, X.L.; investigation, T.G.; resources, J.T.; data curation, T.G.; writing—original draft preparation, T.G. and X.L.; writing—review and editing, C.L. and J.H.; visualization, X.L.; supervision, C.L. and J.H.; project administration, C.L. and J.H.; funding acquisition, J.H. All authors have read and agreed to the published version of the manuscript.

Funding: This work received financial support from the Projects of International Cooperation and Exchanges NSFC (No. 21961142006).

Conflicts of Interest: The authors declare no conflict of interest.

References

1. Burgess, S.K.; Leisen, J.E.; Kraftschik, B.E.; Mubarak, C.R.; Kriegel, R.M.; Koros, W.J. Chain Mobility, Thermal, and Mechanical Properties of Poly(ethylene furanoate) Compared to Poly(ethylene terephthalate). *Macromolecules* **2014**, *47*, 1383-1391, doi:10.1021/ma5000199.
2. Casanova, O.; Iborra, S.; Corma, A. Biomass into chemicals: One pot-base free oxidative esterification of 5-hydroxymethyl-2-furfural into 2, 5-dimethylfuroate with gold on nanoparticulated ceria. *J Catal* **2009**, *265*, 109-116, doi:10.1016/j.jcat.2009.04.019.
3. Jia, W.; Chen, J.; Yu, X.; Zhao, X.; Feng, Y.; Zuo, M.; Li, Z.; Yang, S.; Sun, Y.; Tang, X.; et al. Toward an integrated conversion of fructose for two-step production of 2, 5-furandicarboxylic acid or furan-2, 5-dimethylcarboxylate with air as oxidant. *Chem Eng J* **2022**, *450*, 138172, doi:10.1016/j.cej.2022.138172.

4. Takei, T.; Akita, T.; Nakamura, I.; Fujitani, T.; Haruta, M. Heterogeneous Catalysis by Gold. *Advances in Catalysis* **2012**, *55*, 1-126, doi:10.1016/B978-0-12-385516-9.00001-6.
5. Davis, S.E.; Houk, L.R.; Tamargo, E.C.; Datye, A.K.; Davis, R.J. Oxidation of 5-hydroxymethylfurfural over supported Pt, Pd and Au catalysts. *Catal Today* **2011**, *160*, 55-60, doi:10.1016/j.cattod.2010.06.004.
6. Zhang, Y.; Cao, Y.; Yan, C.; Liu, W.; Chen, Y.; Guan, W.; Wang, F.; Liu, Y.; Huo, P. Rationally designed Au-ZrO_x interaction for boosting 5-hydroxymethylfurfural oxidation. *Chem Eng J* **2023**, *459*, 141644, doi:10.1016/j.cej.2023.141644.
7. Yang, W.; Fu, M.; Yang, C.; Zhang, Y.; Shen, C. Au^{-}–O_v–Ti^{3+}: Active site of MO -Au/TiO_2 catalysts for the aerobic oxidation of 5-hydroxymethylfurfural. *Green Energy & Environment* **2023**, *8*, 785-797, doi:10.1016/j.gee.2021.09.006.
8. Taarning, E.; Nielsen, I.S.; Egeblad, K.; Madsen, R.; Christensen, C.H. Chemicals from Renewables: Aerobic Oxidation of Furfural and Hydroxymethylfurfural over Gold Catalysts. *ChemSusChem* **2008**, *1*, 75-78, doi:10.1002/cssc.200700033.
9. Buonerba, A.; Impemba, S.; Litta, A.D.; Capacchione, C.; Milione, S.; Grassi, A. Aerobic Oxidation and Oxidative Esterification of 5-Hydroxymethylfurfural by Gold Nanoparticles Supported on Nanoporous Polymer Host Matrix. *ChemSusChem* **2018**, *11*, 3139-3149, doi:10.1002/cssc.201801560.
10. Dimitratos, N.; Villa, A.; Wang, D.; Porta, F.; Su, D.; Prati, L. Pd and Pt catalysts modified by alloying with Au in the selective oxidation of alcohols. *J Catal* **2006**, *244*, 113-121, doi:10.1016/j.jcat.2006.08.019.
11. Song, F.; Cen, S.; Wan, C.; Wang, L. Nano-Au Anchored in Organic Base Group-Grafted Silica Aerogel: A Durable and Robust Catalysts for Green Oxidative Esterification of Furfural. *ChemCatChem* **2022**, *14*, e202200704, doi:10.1002/cctc.202200704.
12. P. Ferraz, C.; Braga, A.H.; Ghazzal, M.N.; Zieliński, M.; Pietrowski, M.; Itabaiana, I.; Dumeignil, F.; Rossi, L.M.; Wojcieszak, R. Efficient Oxidative Esterification of Furfural Using Au Nanoparticles Supported on Group 2 Alkaline Earth Metal Oxides. *Catalysts* **2020**, *10*, 430, doi:10.3390/catal10040430.
13. Ren, J.; Mebrahtu, C.; Palkovits, R. Ni-based catalysts supported on Mg–Al hydrotalcites with different morphologies for CO_2 methanation: exploring the effect of metal–support interaction. *Catalysis Science & Technology* **2020**, *10*, 1902-1913, doi:10.1039/c9cy02523e.
14. Dębek, R.; Radlik, M.; Motak, M.; Galvez, M.E.; Turek, W.; Da Costa, P.; Grzybek, T. Ni-containing Ce-promoted hydrotalcite derived materials as catalysts for methane reforming with carbon dioxide at low temperature – On the effect of basicity. *Catal Today* **2015**, *257*, 59-65, doi:10.1016/j.cattod.2015.03.017.
15. Liu, H.; Jia, W.; Yu, X.; Tang, X.; Zeng, X.; Sun, Y.; Lei, T.; Fang, H.; Li, T.; Lin, L. Vitamin C-Assisted Synthesized Mn–Co Oxides with Improved Oxygen Vacancy Concentration: Boosting Lattice Oxygen Activity for the Air-Oxidation of 5-(Hydroxymethyl)furfural. *ACS Catalysis* **2021**, *11*, 7828-7844, doi:10.1021/acscatal.0c04503.
16. Liao, Y.; Yan, H.; Zhou, J.; Yue, Y.; Sun, Y.; Peng, T.; Yuan, X.; Zhou, X.; Liu, Y.; Feng, X.; et al. Interfacial $Au^{\delta-}$-Ov-Zr^{3+} structure promoted C H bond activation for oxidative esterification of methacrolein to Methyl methacrylate. *Chem Eng J* **2023**, *454*, 140322, doi:10.1016/j.cej.2022.140322.
17. Sankar, M.; He, Q.; Engel, R.V.; Sainna, M.A.; Logsdail, A.J.; Roldan, A.; Willock, D.J.; Agarwal, N.; Kiely, C.J.; Hutchings, G.J. Role of the Support in Gold-Containing Nanoparticles as Heterogeneous Catalysts. *Chem Rev* **2020**, *120*, 3890-3938, doi:10.1021/acs.chemrev.9b00662.
18. Wojcieszak, R.; Ferraz, C.; Sha, J.; Houda, S.; Rossi, L.; Paul, S. Advances in Base-Free Oxidation of Bio-Based Compounds on Supported Gold Catalysts. *Catalysts* **2017**, *7*, 352, doi:10.3390/catal7110352.
19. Wei, Y.; Zhang, Y.; Chen, Y.; Wang, F.; Cao, Y.; Guan, W.; Li, X. Crystal Faces-Tailored Oxygen Vacancy in Au/CeO_2 Catalysts for Efficient Oxidation of HMF to FDCA. *ChemSusChem* **2021**, *15*, e202101983, doi:10.1002/cssc.202101983.
20. Zhao, D.; Sheng, G.; Hu, J.; Chen, C.; Wang, X. The adsorption of Pb(II) on Mg_2Al layered double hydroxide. *Chem Eng J* **2011**, *171*, 167-174, doi:10.1016/j.cej.2011.03.082.